Available online at www.sciencedirect.com
SCIENCE DIRECT®
C. R. Physique 5 (2004) 239–248
COMPTES RENDUS PHYSIQUE

Gas phase molecular spectroscopy/Spectroscopie moléculaire en phase gazeuse

Spectroscopy of acetylene Rydberg states studied by VUV absorption and (3 + 1)-Resonantly Enhanced Multiphoton Ionisation

Séverine Boyé [a], Andrea Campos [b], Jean-Hugues Fillion [c], Stéphane Douin [a], Niloufar Shafizadeh [a], Dolores Gauyacq [a,*]

[a] *Laboratoire de photophysique moléculaire, CNRS UPR 3361, bâtiment 210, Université de Paris-Sud, 91405 Orsay cedex, France*
[b] *Instituto de Criminalística Carlos Éboli, Rua Pedro I, no 28 – Centro, Rio de Janeiro, RJ, Brazil*
[c] *LERMA-LAMAp, UMR 8112 du CNRS, Observatoire de Paris & Université de Cergy-Pontoise, 5, mail Gay-Lussac, 95031 Cergy-Pontoise cedex, France*

Presented by Guy Laval

Abstract

The ungerade $ns + nd$ Rydberg states of C_2H_2 converging to the ground state of the $C_2H_2^+$ cation have been investigated in the energy range 74 000–88 000 cm^{-1} by (3 + 1)-multiphoton ionisation (REMPI) and by VUV absorption spectroscopy at the Super-ACO synchrotron radiation facility. Both methods have allowed the selective analysis of the Rydberg transitions with rotational resolution. Mulliken's semi-united atom model, in which predissociation has been taken into account, was used to understand the relative three-photon intensities among the different electronic transitions within the same Rydberg supercomplex. Lifetimes have been evaluated and illustrate very different behaviours towards predissociation for the observed Rydberg states. ***To cite this article: S. Boyé et al., C. R. Physique 5 (2004).***

Résumé

Spectroscopie des états de Rydberg de l'acétylène étudiés par absorption VUV et ionisation multiphotonique résonante à (3 + 1)-photons. Nous avons étudié les états de Rydberg ungerade $ns + nd$ de l'acétylène convergeant vers l'état fondamental du cation $C_2H_2^+$ dans le domaine d'énergie 74 000–88 000 cm^{-1} par ionisation multiphotonique résonante à (3 + 1)-photons et par absorption VUV au rayonnement synchrotron. Ces deux méthodes ont permis d'analyser sélectivement les transitions de Rydberg avec une résolution rotationnelle. Le modèle de l'atome semi-uni de Mulliken a permis d'interpréter les spectres à trois photons des transitions électroniques d'un même supercomplexe de Rydberg en y incluant la prédissociation. Des comportements très variés sont observés dans la prédissociation de ces états à travers l'évaluation de leurs durées de vie. ***Pour citer cet article : S. Boyé et al., C. R. Physique 5 (2004).***

Keywords: VUV; Acetylene; Rydberg state; REMPI; Simulations; Semi-united atom; Predissociation

Mots-clés : VUV ; Acétylène ; État de Rydberg ; IMPR ; Simulations ; Atome semi-uni ; Prédissociation

* Corresponding author.
E-mail address: dolores.gauyacq@ppm.u-psud.fr (D. Gauyacq).

1631-0705/$ – see front matter
doi:10.1016/j.crhy.2004.01.012

1. Introduction

High-resolution molecular spectroscopy from the VUV to the XUV range, 200–50 nm, is very important in the understanding of photon-induced mechanisms in many fields such as for instance in astrophysical media (interstellar medium, cometary atmospheres and circumstellar envelopes) [1]. This spectroscopy usually concerns electronic transitions towards super-excited states including singly excited Rydberg states and doubly excited valence states. Molecular photoabsorption spectroscopic studies, as well as photoionisation and photoelectron studies, have gained new insights from the recent development of high-resolution sources such as synchrotron radiation facilities (see, for instance, [2]) and tuneable XUV and VUV lasers [3,4]. For instance, a broadly tuneable extreme UV laser source has been developed by Hollenstein et al. [3] with a bandwidth of 0.008 cm^{-1} and has been applied to study high Rydberg states of rare gas atoms.

Nevertheless, since highly excited molecular states frequently undergo relaxation towards dissociation or internal conversion in the case of large molecules, the actual spectral resolution needed in the spectral analysis is most often limited by the natural lifetime of these excited states. The useful resolution therefore lies in the sub-wavenumber range (1 to 0.1 cm^{-1}) enabling us to resolve the rotational structure of the electronic transitions.

A second important aspect when dealing with highly excited molecular states is the unavoidable large density of states usually occurring in the region below the first ionisation potential (IP). Indeed, numerous overlapping Rydberg and valence transitions with their vibrational and rotational structures, most often superimposed on underlying dissociation continua, occur in the same spectral range. This is why selective methods have been developed in the last decades to extract valuable information on the structure and stability of high molecular electronic states. Selectivity can be achieved either in the excitation mechanism or in the detection process. For instance, Rydberg state analysis has greatly benefited from the use of selective ionisation techniques as one- or two-colour resonantly-enhanced multiphoton ionisation (REMPI) [5]. Dissociative excited states have been studied in great details by translational fragment spectroscopy [6,7] or by fragment fluorescence excitation spectroscopy [8]. Rotational spectral simplification has also been extensively applied by using supersonic molecular beam expansions.

The present article gives an example of rotationally resolved spectroscopy of *ungerade* acetylene C_2H_2 Rydberg states in the range 74 000–88 000 cm^{-1}, studied by means of complementary techniques: laser-based one-colour $(3+1)$-photon REMPI, synchrotron-based VUV absorption, and fragment fluorescence detection. The spectral range presently studied is limited to transitions below the first IP of acetylene, i.e., 91 956 cm^{-1}. Therefore the only relaxation mechanism to be considered is predissociation into neutral fragments (C_2H, C_2, CH, ...). We have observed a competition between this process and ionisation in the REMPI experiment [9].

After describing the observed spectra of acetylene (three-photon and one-photon), spectral simulations are presented in detail, including relative electronic transition intensities and rotational profiles. Such simulations allowed us to confirm the vibronic symmetries of the upper states, and the validity of the semi-united atom approximation. Predissociation has been included in the simulations to interpret both experimental linewidths and ionisation signal intensities. Finally, lifetimes for the observed Rydberg states of acetylene could be extracted from such an analysis.

2. Experimental section

The $(3+1)$-REMPI experiment was performed in a magnetic bottle photoelectron spectrometer described elsewhere [10]. Acetylene was introduced into a vacuum chamber through a 2-mm diameter hole. The typical background pressure was 10^{-5} mbar in the interaction region, so that an effusive beam condition allowed for moderate rotational cooling of the molecules (150 K-typical rotational temperature). Tuneable radiation was generated by an excimer (XeCl, LUMONICS PM 886) pumped dye laser (Lambda Physik FL2002) operating in the 360–404 nm spectral region (BMQ, DMQ, QUI, PBBO dye solutions), with a 0.3 cm^{-1} bandwidth. The beam was focused with a 150-mm focal length lens. Beam intensities were maintained below 500 μJ per pulse and monitored during the scan by a micro Joulemeter (Laser Precision Corporation RjP 700). Spectral wavelength calibration was achieved by recording simultaneously the neon optogalvanic signal from a Fe–Ne hollow cathode. The REMPI signal was collected as a function of laser wavelength and accumulated over c.a. 30 laser shots.

The one-photon VUV absorption spectrum of C_2H_2 was performed at the synchrotron radiation facility in Orsay (Super-ACO) by using two beamlines, SA63 or SU5. The SA63 beam line is equipped with a 3-m Eagle normal incidence monochromator and 1800 grooves/mm grating tuned in the 153–105 nm spectral region with a 0.08 nm resolution. In the experiment performed with this beam line, acetylene was excited within cell conditions, at a pressure of 10^{-4} mbar. The SU5 beam light, dispersed by a high-resolution 6.65 m Eagle off-plane normal incidence monochromator and a 2400 grooves/mm grating was tuned in the 117.5–116.9 nm energy range with a resolution of about 0.0012 nm [2]. In this case, pure acetylene was introduced in a supersonic jet expansion through a 50-μm nozzle (35 K-mean rotational temperature).

The absorption signal was obtained by detecting the transmitted light (through the visible fluorescence of a coated sodium salicylate window by a photomultiplier tube Hamamatsu R928) with and without acetylene gas.

In the experiment performed on the SU5 beamline at the synchrotron radiation, the low density of molecules in the molecular beam precluded observation of highly resolved absorption spectrum, while the fluorescence excitation signal led to a much better signal to noise. The isotropic visible fluorescence of the fragments was collected by an ellipsoidal mirror system coupled to a bundle of fused silica fibres which guided the signal onto a photomultiplier tube (Hamamatsu R928) [11].

3. Observation of the Rydberg states of acetylene in the VUV range

Rydberg states of acetylene converging to the $\widetilde{X}^2\Pi_u$ ground state of $C_2H_2^+$ are linear ($D_{\infty h}$ symmetry group) and can be classified into two vibronic symmetry species: the *ungerade* and the *gerade* states. *Ungerade* states can be observed through excitation with an odd number of photons while *gerade* states can only be observed through an even number of photons with the same or with different wavelengths. The singlet *ungerade* states have been the subject of numerous investigations, both experimental (see, e.g., [12,13] and references therein) and theoretical [14–16]. Many UV absorption bands involving the $ns\sigma_g$, $^1\Pi_u$ and $nd\delta_g$, $^1\Pi_u$ series for the four isotopomers C_2H_2, C_2D_2, $^{13}C_2H_2$ and C_2HD have been rotationally analysed. Some other Rydberg transitions appear completely diffuse for all n values [17,13] (e.g., $nd\sigma_g$, $^1\Pi_u$ and $nd\pi_g$, $^1\Sigma_u^+$ series).

Fig. 1(a) displays a low-resolution absorption spectrum of acetylene extending from the lowest $3s$ Rydberg state up to the IP, and recorded with synchrotron radiation (SA63 beamline). In addition to the origin bands, progressions in the ν_2 C–C stretching mode are observed, as expected for a linear geometry almost identical to the geometry of the ground state cation. The complete origin band series displays an intensity variation following a textbook $1/n^3$ scaling law where n is the principal quantum number. Although the experimental bandwidth of the spectrum in Fig. 1(a) does not allow resolving the rotational structure, some manifestations of different predissociation decay rates show up in this spectrum. For instance the $2_0^1\ 3s\sigma\,^1\Pi_u - \widetilde{X}$ band at 67640 cm^{-1} exhibits a broad structure of c.a. 270 cm^{-1} FWHM, about six times larger than the experimental bandwidth, indicative of a very short lifetime of c.a. 20 fs. On the other hand, although most of the Rydberg states are predissociated, some of them have a lifetime longer than 10 ps, allowing observation of single rotational lines. The enlarged spectrum of panel (a) recorded on the SU5 high resolution beamline (0.9 cm^{-1} spectral bandwidth) shows an intermediate situation on the $\tilde{I}^1\Pi_u - \widetilde{X}^1\Sigma_g^+$ origin band with rotationally resolved structure, only slightly broaden by predissociation. This spectrum has been recorded through the visible fluorescence of the dissociation products of acetylene. Indeed, since acetylene is transparent in the visible, visible emission only arises from excited neutral fragments produced by the Rydberg states dissociation. Such a fluorescence excitation spectrum should reproduce the absorption spectrum as long as the predissociation is independent from the rotational quantum number, which has been checked in our spectra [18].

Among other experiments involving odd number of photons in the excitation process, REMPI studies performed with one-colour, three-photon excitation have been carried out on *ungerade* Rydberg states [19–22,9]. These experiments have provided a new wealth of information about acetylene Rydberg states, and especially about new electronic symmetries. This is shown in the panoramic $(3+1)$-REMPI spectrum of Fig. 1(b).

The observed REMPI intensity of panel (b) deserves some comments. By comparison with the absorption spectrum of panel (a), one can clearly see that the relative REMPI intensity of the Rydberg series decreases much faster than the expected $1/n^3$ law. This drastic decrease results mainly from competition between predissociation and ionisation of the Rydberg states with increasing excitation energy. This gives a limitation to the REMPI method applied to highly excited molecular states. The second limitation of such a one-colour REMPI study is inherent to the density of states in the high-energy region below IP.

In the low energy region between 74 000 and 77 000 cm^{-1}, the REMPI structure corresponds to excitation of the $\widetilde{D}$ and $\widetilde{F}$ Rydberg state as well as to the $\widetilde{E}$ valence state [23]. Observation of valence states by such a REMPI technique is very rare, due to the forbidden ionisation step, unless a very strong Rydberg-valence mixing occurs as it is the case here for the $\widetilde{E}$ and $\widetilde{F}$ states.

The relatively good laser bandwidth (0.3 cm^{-1}) allowed us to observe the rotational structure of new electronic bands and to extract predissociation bandwidths for single rotational lines. Two examples ($\tilde{I}^1\Pi_u - \widetilde{X}^1\Sigma_g^+$ origin band and $\widetilde{H'}^1\Delta_u - \widetilde{X}^1\Sigma_g^+$ ν_2 band) are shown in the enlarged spectra of Fig. 1(b).

To conclude about this overview of *ungerade* Rydberg states of acetylene, the REMPI technique can be considered as very complementary to absorption techniques, since it is selective towards observation of Rydberg states only, with much greater variety of electronic symmetry. On the other hand, relaxation processes, which are common in this highly excited region, compete with ionisation and lead to a weaker REMPI signal. A third complementary technique is the dissociation spectroscopy observed for instance via fragment fluorescence excitation spectra (as shown in the insert of Fig. 1(a)), as it has been successfully applied for the high gerade Rydberg states of acetylene [24].

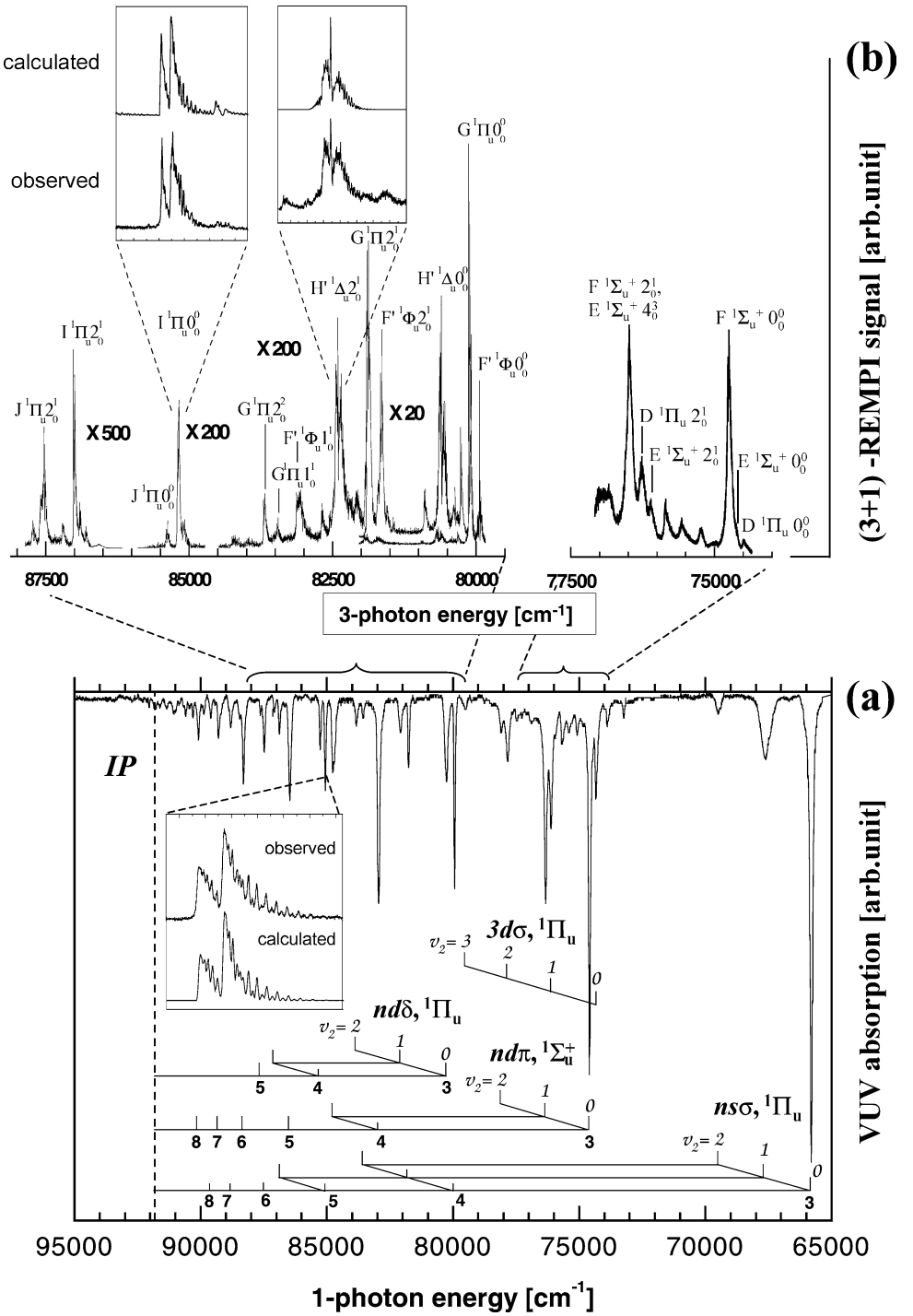

Fig. 1. (a): One-photon absorption spectrum of acetylene Rydberg states in the range 65 000–95 000 cm^{-1} recorded on the SA63 synchrotron beamline (bandwidth 0.1 nm). In the insert is displayed a spectrum of the rotationally resolved $\tilde{I}\ 5s\sigma,\ ^1\Pi_u\ 0_0^0$ band taken on the SU5 beamline with a much higher resolution (0.0012 nm). (b): (3 + 1)-photon REMPI spectrum of acetylene in the range 74 000–88 000 cm^{-1}. This spectrum is a composite of several laser scans with different dye solutions. Approximate multiplying factors are given with respect to the one at 80 000 cm^{-1}. The enlarged spectra displayed in the two inserts of this panel exhibit rotational structure for the origin band of $\tilde{I}5s\sigma,\ ^1\Pi_u$ state and the ν_2 band of $\tilde{H}'3d\pi\ ^1\Delta_u$ state.

4. Methods of analysis and simulations

4.1. Rotational profiles

Analysis of $(n+1)$-REMPI spectra is based on the separability of the photoionisation process into two steps: n-photon absorption to the resonant excited state of interest, followed by one-photon ionisation. In these experiments, the ionisation step is most often saturated in such a way that the overall REMPI transition probability is governed by the initial n-photon absorption step.

Dixon et al. [25] have presented a unified treatment for the calculation of the multiphoton line strengths for molecules belonging to a variety of point groups. Some important aspects of this treatment are described below, as they are relevant to the three-photon REMPI spectra of acetylene.

Application of Fermi's golden rule leads to the following expression of the transition probability for three-photon absorption:

$$\Gamma \propto \left|\mathrm{T}(\varepsilon)\cdot\left\langle\Psi'\middle|T(B)\middle|\Psi''\right\rangle\right|^2\rho(E), \tag{1}$$

where $\rho(E)$ is the final density of states, and where $T(\varepsilon)$ and $\langle\Psi'|T(B)|\Psi''\rangle$ are the third rank Cartesian light polarisation tensor and the hyperpolarisability transition matrix element, respectively.

The transition operator can be handled elegantly by expressing it in a spherical coordinate representation, which leads to a limited tensor expansion in the case of three equivalent photons: $T(B)\equiv T^3(B)+T^1(B)$. Each T^k tensor possesses $2k+1$ components, T^k_p, in the space-fixed system (with $p=k,k-1,\ldots,-k$). We shall write the rovibronic wavefunctions using combination of the rotational basis functions $|JM\Lambda\rangle$, conforming to Hund's case (b):

$$|\Psi\rangle = d/\sqrt{2}\big[|\eta\ JM\Lambda\rangle+\alpha|\eta\ JM-\Lambda\rangle\big],$$

where η are vibronic quantum numbers, and where $d=\sqrt{2}$ and $\alpha=0$ for Σ states ($\Lambda=0$), or $d=1$ and $\alpha=\pm1$ for e/f states (Λ^+/Λ^-).

In a second step, the $T^k_p(B)$ components are projected over the molecular-fixed components $T^k_q(B)$ using frame transformation matrix elements [25]. After summation over the M sub-levels, and after simplifications arising from the properties of Wigner rotation functions and from the $(3-j)$ Wigner symbols orthogonality, the intensity line strength is given by:

$$\begin{aligned}
I_{\Lambda'\Lambda''}(J'J'') \propto{}& N(T,J'')(2J'+1)(2J''+1)\big\{1-(-1)^{\Delta J}\alpha'\alpha''\big\}^2\sum_{k=1,3}\left[\sum_p\frac{|T^k_{-p}(\varepsilon)|^2}{2k+1}\right]\\
&\times\sum_{q,q'}\left\{\left|\left\langle\eta'\middle|T^k_q(B)\middle|\eta''\right\rangle\right|^2\begin{pmatrix}J'&k&J''\\-\Lambda'&q&\Lambda''\end{pmatrix}^2+\left|\left\langle\eta'\middle|T^k_{q'}(B)\middle|\eta''\right\rangle\right|^2\begin{pmatrix}J'&k&J''\\-\Lambda'&q'&-\Lambda''\end{pmatrix}^2\right.\\
&\left.+2\alpha''\left\langle\eta'\middle|T^k_q(B)\middle|\eta''\right\rangle\left\langle\eta'\middle|T^k_{q'}(B)\middle|\eta''\right\rangle\begin{pmatrix}J'&k&J''\\-\Lambda'&q&\Lambda''\end{pmatrix}\begin{pmatrix}J'&k&J''\\-\Lambda'&q'&-\Lambda''\end{pmatrix}\right\}\\
&(\text{with }\Lambda'\geqslant0\text{ and }\Lambda''\geqslant0).
\end{aligned}\tag{2}$$

In Eq. (2), $N(T,J'')$ is the temperature dependent rotational population including the nuclear statistic weight factors of the initial ground state. The $(3-j)$ symbols are the generalisation of the kth rank tensor of the Hönl–London line strength factor for one-photon transition (described with $k=1$). They hold the selection rules $\Delta J=0,\pm1,\ldots,\pm3$ and $\Delta\Lambda=\pm q$. This expression has been incorporated into a band-simulation computer program that includes the appropriate rotational constants of the levels of interest and a line-shape function.

Because of the $\Delta\Lambda$ selection rules, observation of Rydberg states excited from the ground state is not restricted to Σ or Π but can reveal a wider range of vibronic symmetries. As an example, Fig. 2 displays several simulated REMPI rotational profiles, depending upon the vibronic symmetry of the lower and excited states. These simulated profiles demonstrate the interest of achieving rotational resolution experimentally, in order to reveal the excited state vibronic symmetry. For example, this approach was used by Fillion et al. [22] to identify the $^1\Delta_u$, $3d\pi$ component of the $3d+4s$ Rydberg supercomplex of acetylene that previously led to a misassignment due to the lack of sufficient spectral resolution.

Transitions that are forbidden by one-photon absorption and allowed by three-photon are entirely carried by a third rank tensor component $T^3_q(B)$. The relative intensities of the rotational lines can therefore be predicted by one $(3-j)$ factor, without fitting any parameter. In this particular case, the relative intensities of the rotational lines are independent of polarisation, since the polarisation tensor is factorised in Eq. (2). On the other hand, transitions which are allowed both by one-photon and three-photon absorption depend on both the first rank $T^1(B)$ and third rank $T^3(B)$ tensors. In this case, the calculation of the band intensity depends also on the relative weight of the tensor components. These relative weights have to be determined by fitting

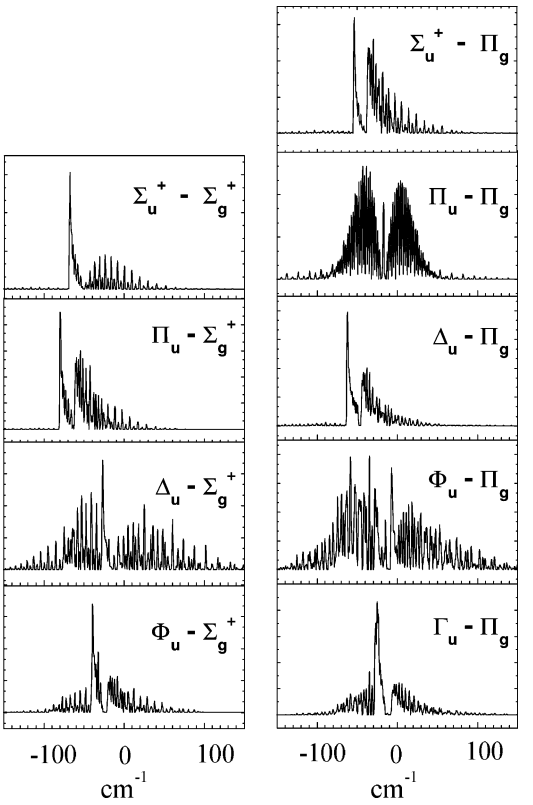

Fig. 2. Rotational structure simulations of the possible electronic transitions reached by a three-photon absorption with a linearly polarised light. A relative weight $T^3/T^1 = 0.3$ has been used for all transitions involving both tensors (see text).

the observed rotational structure with Eq. (2). In particular, the observed rotational branches with $|\Delta J| \geqslant 2$ provide the value of the third rank tensor. This is another demonstration that rotational resolution is crucial in the analysis of REMPI spectra. When both T^1 and T^3 tensors are involved, the multiphoton absorption is polarisation dependent. As shown in Eq. (2), the weight of the $T_q^k(B)$ components is governed by the magnitudes of the polarisation tensor $T_p^k(\varepsilon)$ components that can be controlled to some extent, by changing the polarisation of the light beam. In particular, the $T^1(B)$ rank contribution can be cancelled by using circularly polarised light [26,27]. This powerful diagnostic has been used in the characterisation of the $4s + 3d$ supercomplex of acetylene [22].

4.2. Semi-united atom approximation

According to Mulliken [28], the electronic properties of a molecule are in many respects similar to those of the corresponding semi-united atom, i.e., the atom having the same number of electrons as the valence electrons of the molecule. In this description, the ten valence electrons of acetylene are compared to those of the neon atom with the following correspondence of their ground state configurations:

$$\text{Ne} \qquad (1s)^2(2s)^2(2p)^6,$$
$$\text{C}_2\text{H}_2 \ldots (2\sigma_g)^2(2\sigma_u)^2(3\sigma_g)^2(1\pi_u)^4.$$

Comparison between these two configurations suggests a 'p' atomic character for the $1\pi_u$ orbital. Therefore, the absorption spectrum of acetylene towards its Rydberg states is expected to be dominated by transitions to ns and nd states, which is indeed the case.

By using the semi-united atom approximation, one can evaluate not only the rotational profile of each Rydberg transition, but also the relative electronic radial + angular transition moments within a given $ns + (n-1)d$ Rydberg supercomplex. This approximation allows us to predict the relative electronic band strengths of all members belonging to the same Rydberg supercomplex, including s and d orbitals.

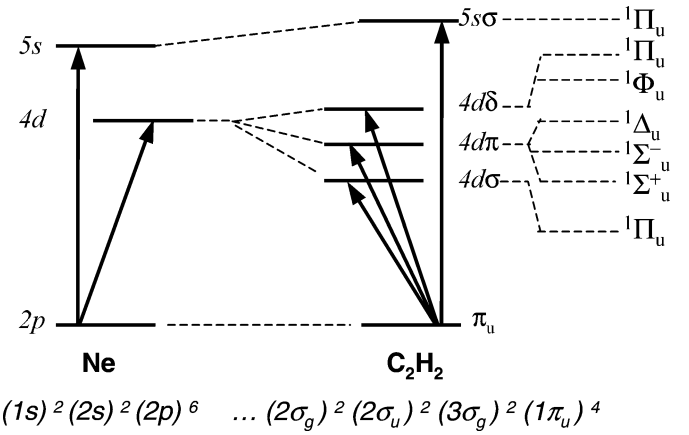

Fig. 3. Schematic diagram of the semi-united atom picture used in the present work to obtain the relative Rydberg transition intensities within the same $5s + 4d$ supercomplex (see text).

Concerning the $5s + 4d$ Rydberg supercomplex, comparison with observed intensities in the absorption spectrum of neon leads to the same radial factor for the electronic transition moments towards the $5s$ and $4d$ levels. As illustrated in Fig. 3, the molecular Rydberg state symmetry has further to be taken into account through an angular electronic factor included in the transition moment. When three-photon excitation is considered, one can still use the semi-united atom approximation in order to predict the relative intensities involving the different members of the $4d$ complex shown on Fig. 3: the $4d\sigma_g(^1\Pi_u)$, $4d\pi_g(^1\Sigma_u^+)$, $4d\delta_g(^1\Pi_u)$, $4d\pi_g(^1\Delta_u)$, and $4d\delta_g(^1\Phi_u)$ Rydberg states. The $4d\pi_g(^1\Sigma_u^-)$ Rydberg state component is also shown on Fig. 3 for completeness, although the transition to this state is three-photon forbidden.

According to the Wigner–Eckart theorem, the semi-united approximation can be incorporated in Eq. (2) presented in Section 4.1 as follows:

$$T_q^k(B) = T^k(B) \begin{pmatrix} \ell' & k & \ell \\ -\lambda' & q & \lambda'' \end{pmatrix}. \tag{3}$$

Within the semi-united atom approximation, the ground state orbital is considered as a pπ orbital with $\ell'' = 1$ and $\lambda'' = \pm 1$. Eq. (3) shows that the only unknown parameters are the radial part of the three-photon transition moment, i.e., $T^k(B)$ $(k = 1, 3)$. The molecular symmetry is taken into account by the electronic and rotational angular factors given by the $(3 - j)$ symbols of Eq. (2).

In the present work, light was linearly polarised, i.e., $p = 0$, leading to polarisation weight factors in Eq. (2) of $1/5$ and $2/35$ for the first-rank tensor and the third-rank tensor contribution, respectively. The ground state $^1\Sigma_g^+$ molecular symmetry is given by $\Lambda'' = 0$.

Fig. 4(a) shows the $3 + 1$ REMPI spectrum of C_2H_2 recorded in the $5s + 4d$ region revealing four Rydberg states: $\tilde{I}\ ^1\Pi_u$ $5s\sigma_g$, $\tilde{J}\ ^1\Pi_u$ $4d\delta_g$, $^1\Phi_u$ $4d\delta_g$ and $^1\Delta_u$ $4d\pi_g$. Simulation of the weak transition to the $^1\Phi_u$ $4d\delta_g$ state involves only the T^3 tensor. According to our model, the intensity of the $^1\Delta_u - {}^1\Sigma_g^+$ transition is governed by the same T^3 tensor. On the other hand, the transition leading to the $\tilde{I}\ ^1\Pi_u$ $5s\sigma_g$ state is only carried by the first rank tensor, as in one-photon absorption. The same T^1 factor is used in the calculation for the $4d$ states of the same supercomplex.

Fig. 4(b) displays the resulting simulated three-photon spectra of the $5s + 4d$ supercomplex obtained by fitting only one parameter, the ratio T^1/T^3 [9].

As shown in Fig. 4, the three-photon transitions to the $^1\Phi_u$ $4d\delta_g$ and $^1\Delta_u$ $4d\pi_g$ states are expected to be weak and are very weak indeed in the observed REMPI spectrum. The $^1\Delta_u$ $4d\pi_g - \tilde{X}\,^1\Sigma_g^+$ transition barely shows up in the red tail of the $\tilde{J} - \tilde{X}$ transition of C_2H_2 (Fig. 4(a)).

4.3. Predissociation effects

Fig. 4 (a) and (b) show the comparison between the experimental three-photon spectrum in the region of the $5s\sigma$, $^1\Pi_u$ and $4d\delta$, $^1\Pi_u$ upper members of the $5s + 4d$ supercomplex, and the calculated spectrum based on the semi-united atom approximation. As was pointed out in Section 4.2, this approximation gives an estimate of the relative electronic transition intensities within the same $5s + 4d$ supercomplex, provided that ionisation is the fastest relaxation channel. Most of the Rydberg states of acetylene undergo a 'slow' dissociation mechanism into $C_2H(A) + H$ fragments, taking place in the picosecond time

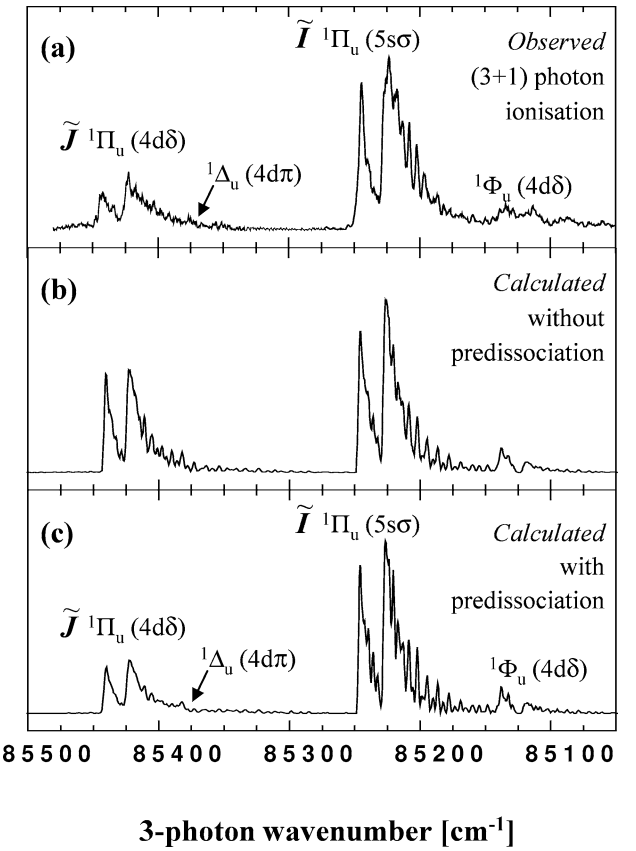

Fig. 4. C_2H_2 Rydberg $5s + 4d$ supercomplex in the 85 300 cm^{-1} region. (a) Observed $(3 + 1)$-photon spectrum; (b) calculated three-photon spectrum using the semi-united atom approximation; (c) simulation of the REMPI spectrum taking into account predissociation effects.

scale [11]. For some accidental cases, as in the $\widetilde{H}^1\Pi_u$, $3d\delta$ state, a very fast dissociation occurs ($\sim$50 fs), ruling out any observation of this state via nanosecond REMPI experiments.

Comparison between intensities of the simulated three-photon spectrum (Fig. 4(b)) and the experimental REMPI spectrum (Fig. 4(a)) indicates that predissociation competes with ionisation, inducing a weakening of the $\tilde{J} - \widetilde{X}$ transition in the REMPI signal. Indeed, in the absence of predissociation, the three-photon $\tilde{J} - \widetilde{X}$ transition is expected to be about 50% weaker than the nearby electronic component $\tilde{I} - \widetilde{X}$ transition. On the other hand, even without invoking predissociation, the intensity of the $^1\Delta_u$ $(4d\pi) - \widetilde{X}^1\Sigma_g^+$ origin band is expected to be weak as compared with the nearby electronic components of the supercomplex, as explained in Section 4.2. above.

In Fig. 4(c), predissociation has been taken into account in the simulation by artificially including a constant damping factor for the ionisation signal as follows:

$$s^i = I^{(3)} \frac{k_i}{k_i + k_p}, \tag{4}$$

where $I^{(3)}$ is given by Eqs. (2) and (3), and where k_i and k_p are the ionisation rate and the predissociation rate of the relevant upper Rydberg state, respectively. The predissociation lifetime is estimated from the observed rotational linewidths after deconvolution by the laser bandwidth. Table 1 summarises the lifetimes derived from this analysis for different Rydberg states.

The ratio $k_i/(k_i + k_p)$ used for the simulations of Fig. 4(c) is 0.5 for $\tilde{J}$ and 1 for all the other upper states ($\tilde{I}\ 5s^1\Pi_u$, $4d^1\Phi_u$ and $4d^1\Delta_u$) leading to an intensity of the $\tilde{J} - \widetilde{X}$ transition divided by a factor of 2, as compared to the other transitions. We have assumed here that the predissociation rate k_p is smaller than the ionisation rate k_i by at least a factor of 10 and can be neglected in Eq. (4), for all transitions except the $\tilde{J} - \widetilde{X}$ transition.

As a conclusion, ionisation and predissociation decay mechanisms can be clearly observed in the REMPI spectra when they compete in the same time scale, as in the example of the $\tilde{J}$ state above.

Table 1
Lifetimes for the electronic components of the lowest $ns + nd$ supercomplexes of C_2H_2 estimated from observed linewidths (the uncertainty on lifetime is of the order of 30%)

	$v_2 = 0$		$v_2 = 1$	
Electronic state	Energy (cm^{-1})	Lifetime	Energy (cm^{-1})	Lifetime
$\widetilde{C}\ 3s\sigma, {}^1\Pi_u$	65 790[a]	∼50 fs[b]	67 640	∼20 fs[b]
$\widetilde{D}\ 3d\sigma, {}^1\Pi_u$	74 500[c]	–	76 480[d]	∼60 fs[d]
$\widetilde{F}\ 3d\pi, {}^1\Sigma_u^+$	74 754[c]	∼100 fs	76 480[d]	∼100 fs[d]
$\widetilde{F}'\ 3d\delta, {}^1\Phi_u$	79 931	> 10 ps[e]	81 695	∼1 ps[f]
$\widetilde{G}\ 4s\sigma, {}^1\Pi_u$	80 111	> 10 ps[g]	81 925	∼3 ps[h]
$\widetilde{H}\ 3d\delta, {}^1\Pi_u$	80 458	75 fs[g]	82 260	60 fs[h]
$\widetilde{H}'\ 3d\pi, {}^1\Delta_u$	80 640	∼2 ps[i]	82 445	∼1 ps[b]
$4d\delta, {}^1\Phi_u$	85 140	–	86 959[e]	–
$\tilde{I}\ 5s\sigma, {}^1\Pi_u$	85 229	∼3 ps[e]	87 054[e]	∼2 ps[a]
$4d\pi, {}^1\Delta_u$	85 367[e]	< 100 fs[b]	–	–
$\tilde{J}\ 4d\delta, {}^1\Pi_u$	85 425	∼2 ps[e]	87 250[e]	∼2 ps[a]

[a] [13], [b] this work, [c] [12], [d] [30], [e] [9], [f] [19], [g] [11], [h] [6], [i] [22].

5. Conclusion

In this article, we have shown that the REMPI technique is a powerful spectroscopic tool for observing low to high-lying molecular Rydberg states with currently achieved rotational resolution. In particular, this technique precludes observation of valence states or superexcited states lying in the same energy region because of the forbidden one-photon ionisation step.

The analysis of the Rydberg transitions of acetylene has been carried out through a careful simulation of the rotational profile in order to characterise the vibronic symmetry of the upper state. A complete and unambiguous assignment of the vibrational Rydberg bands also needs measurements on the deuterated acetylene C_2D_2 which have not been shown in this paper (see, for instance, [22]). The semi-united atom approximation introduced by Mulliken [28] has allowed us to understand the strong differences among the various electronic transitions intensities within the same Rydberg supercomplex, and to separate the role of predissociation from intrinsic three-photon transition moments effects.

The limitation of the REMPI approach is the strong competition between ionisation and dissociation experienced by some Rydberg states. When both relaxation channels take place in the same time scale, REMPI can lead to a good estimate of the predissociation rate. When predissociation is one or two orders of magnitude faster than ionisation, alternative techniques have to be used such as H-atom fragment translational spectroscopy [7,6] or fluorescence detection of the neutral fragments [29,11].

Acknowledgements

This work was supported by the Programme de Physique et Chimie du Milieu Interstellaire (PCMI) and the Programme National de Planétologie (PNP).

References

[1] A.E. Glassgold, Annu. Rev. Astron. Astrophys. 34 (1996) 241–277.
[2] L. Nahon, C. Alcaraz, J.L. Marlats, B. Lagarde, F. Polack, R. Thissen, D. Lepère, K. Ito, Rev. Sci. Instr. 72 (2001) 1320–1329.
[3] U. Hollenstein, H. Palm, F. Merkt, Rev. Sci. Instr. 71 (2000) 4023–4028.
[4] W. Ubachs, K.S.E. Eikema, W. Hogevorst, P.C. Cacciani, J. Opt. Soc. Am. B 14 (1997) 2469–2476.
[5] W.Y. Cheung, W.A. Chupka, S.D. Colson, D. Gauyacq, P. Avouris, J.J. Wynne, J. Chem. Phys. 78 (1983) 3625–3634.
[6] P. Löffler, D. Lacombe, A. Ross, E. Wrede, L. Schnieder, K.H. Welge, Chem. Phys. Lett. 252 (1996) 304–310.
[7] D.H. Mordaunt, M.N.R. Ashfold, R.N. Dixon, P. Löffler, L. Schnieder, K.H. Welge, J. Chem. Phys. 108 (1998) 519–525.
[8] Y.C. Hsu, M.S. Lin, C.P. Hsu, J. Chem. Phys. 94 (1991) 7832–7841.
[9] A. Campos, S. Boyé, S. Douin, C. Fellows, J.H. Fillion, N. Shafizadeh, D. Gauyacq, J. Phys. Chem. A 105 (2001) 9104–9110.
[10] S. Guizard, N. Shafizadeh, M. Horani, D. Gauyacq, J. Chem. Phys. 94 (1991) 7046–7060.
[11] S. Boyé, A. Campos, S. Douin, C. Fellows, D. Gauyacq, N. Shafizadeh, P. Halvick, M. Boggio-Pasqua, J. Chem. Phys. 116 (2002) 8843–8855.

[12] M. Herman, R. Colin, J. Mol. Spectrosc. 85 (1981) 449–461.
[13] M. Herman, R. Colin, Phys. Scr. 25 (1982) 275–290.
[14] D. Demoulin, Chem. Phys. 11 (1975) 329–341.
[15] M. Peric, R.J. Buenker, S.D. Peyerimhoff, Mol. Phys. 53 (1984) 1177–1193.
[16] K. Malsh, R. Rebentisch, P. Swiderek, G. Hohlneicher, Theor. Chem. Acc. 100 (1998) 171–182.
[17] R. Colin, M. Herman, I. Kopp, in: Proceedings of the 21st Liège Int. Astrophysical Symp., 1977, pp. 355–384.
[18] A. Campos, S. Boyé, P. Bréchignac, S. Douin, C. Fellows, N. Shafizadeh, D. Gauyacq, Chem. Phys. Lett. 314 (1999) 91–100.
[19] M.N.R. Ashfold, R.N. Dixon, J.D. Price, B. Tutcher, Mol. Phys. 56 (1985) 1185–1199.
[20] M.N.R. Ashfold, C.D. Heryet, J.D. Prince, B. Tutcher, Chem. Phys. Lett. 131 (1986) 291–297.
[21] T. Orlando, S.L. Anderson, J.R. Appling, M.G. White, J. Chem. Phys. 87 (1987) 852–860.
[22] J.H. Fillion, A. Campos, J. Pedersen, N. Shafizadeh, D. Gauyacq, J. Chem. Phys. 105 (1996) 22–30.
[23] V. Blanchet, S. Boyé, S. Zamith, A. Campos, B. Girard, J. Liévin, D. Gauyacq, J. Chem. Phys. 119 (2003) 3751–3762.
[24] K. Tsuji, N. Arakawa, A. Kawai, K. Shibuya, J. Phys. Chem. A 106 (2002) 747–753.
[25] R.N. Dixon, J.M. Bayley, M.N.R. Ashfold, Chem. Phys. 84 (1984) 21–34.
[26] M.N.R. Ashfold, J.M. Bayley, R.N. Dixon, Chem. Phys. 84 (1984) 35–50.
[27] M.N.R. Ashfold, Mol. Phys. 58 (1986) 1–20.
[28] R.S. Mulliken, Int. J. Quant. Chem. 1 (1967) 103.
[29] J.C. Han, C. Ye, M. Suto, L.S. Lee, J. Chem. Phys. 90 (1989) 4000–4007.
[30] P. Löffler, E. Wrede, L. Schnieder, J.B. Halpern, W.M. Jackson, K.H. Welge, J. Chem. Phys. 109 (1998) 5231–5246.